Environmental Science Processes & Impacts

ROYAL SOCIETY OF CHEMISTRY

PAPER

View Article Online
View Journal | View Issue

Cite this: *Environ. Sci.: Processes Impacts*, 2026, **28**, 1299

Manganese oxide-mediated halogenation of carbazole under marine-related conditions

Meng Zhang,[ab] Jia Tang[a] and Kunde Lin *[a]

Polyhalogenated carbazoles (PHCZs) are emerging halogenated organic compounds detected in various environmental matrices, including marine environments. However, the origins of PHCZs are not yet fully understood. This study investigates the manganese oxide-mediated transformation of carbazole into PHCZs under marine-related conditions. Brominated and chlorinated carbazoles were produced through manganese oxide-mediated oxidation of carbazole in the presence of halide ions, with brominated carbazoles being the dominant species. Both reactive bromine species (RBS) and reactive chlorine species were detected in the reaction system. However, the detected RBS concentration was much lower than that of the observed brominated carbazoles under identical conditions. In reactions spiked with *tert*-butanol and methanol as $^{\bullet}OH$ scavengers, RBS production decreased from 0.56 nmol L^{-1} to 0.12 nmol L^{-1}, while the yield of 3-BCZ increased. These results suggest that PHCZ formation occurs through two primary pathways: (i) electrophilic substitution, where reactive halogen species generated by manganese oxide-mediated oxidation of halide ions react with carbazole and (ii) nucleophilic addition, where halide ions attack carbazole cations formed *via* manganese oxide oxidation. Our findings provide new insights into the abiotic processes contributing to the environmental load of PHCZs and suggest that manganese oxides play a critical role in the biogeochemical cycling of halogenated organic compounds in coastal and marine ecosystems.

Received 23rd January 2026
Accepted 16th March 2026

DOI: 10.1039/d6em00064a

rsc.li/espi

Environmental significance

Polyhalogenated carbazoles (PHCZs) are emerging persistent organic pollutants frequently detected in marine and coastal environments, yet their natural formation pathways remain poorly understood. This study demonstrates that δ-MnO_2, a ubiquitous and highly reactive manganese oxide in marine sediments, can mediate the abiotic halogenation of carbazole under environmentally relevant conditions. By revealing mineral-driven halogenation as a previously overlooked natural source of PHCZs, this work provides new insights into the geochemical processes governing the environmental occurrence of halogenated organic pollutants. These findings highlight the important role of manganese oxides in shaping the environmental fate of halogenated compounds and suggest that mineral-mediated reactions may contribute to the background levels of PHCZs in marine ecosystems.

1 Introduction

Polyhalogenated carbazoles (PHCZs) are a class of emerging persistent organic pollutants that have gained increasing attention due to their widespread occurrence and potential ecological risks. To date, more than 30 PHCZ congeners have been identified in diverse environmental matrices, including sediments,[1–5] soils,[6–8] air,[8–10] water,[5,8] and biological samples worldwide.[8,11,12] Structurally similar to polychlorinated dibenzofurans, PHCZs exhibit notable bioaccumulation potential and environmental persistence.[11,13,14] Moreover, toxicological studies have shown that PHCZs can induce developmental toxicity,[15,16] neurotoxicity,[16,17] and endocrine-disrupting effects,[18,19] highlighting their significance in environmental and public health concerns.

Understanding the environmental sources and formation mechanisms of PHCZs is essential for assessing their environmental fate and risks. Both anthropogenic and natural processes have been proposed to explain their ubiquitous presence. Industrial activities can lead to unintended generation and release of PHCZs.[20–22] For example, Sun *et al.* identified and quantified PHCZ emissions from 13 major industrial sectors in China, revealing that coke production is the dominant source (9229 g per year), followed by iron ore sintering facilities (3237 g per year).[23] Additionally, Zhang and Lin reported that advanced oxidation processes used in coking wastewater treatment can generate PHCZs as byproducts.[24] However, these anthropogenic sources alone fail to explain the presence of PHCZs in sediment cores predating large-scale industrial activities,[2,3,25] suggesting that natural formation pathways also play a critical role. Indeed, natural halogenation

[a]*Fujian Provincial Key Laboratory for Coastal Ecology and Environmental Studies, College of the Environment and Ecology, Xiamen University, Xiamen 361102, China. E-mail: link@xmu.edu.cn*

[b]*National Academy of Forestry and Grassland Administration, Beijing 102600, China*

processes have been demonstrated as a plausible source of PHCZs. Laboratory studies have shown that carbazole can undergo enzymatic halogenation catalyzed by chloroperoxidase and bromoperoxidase, resulting in the formation of a variety of chlorinated, brominated, and mixed-halogenated carbazoles.[12,26] These findings highlight that natural oxidative halogenation may substantially contribute to the environmental burden of PHCZs, especially in marine systems rich in halide ions.

Manganese oxides represent another important, yet less explored, natural halogenation mediator. As ubiquitous and powerful oxidants in soils and marine sediments, manganese oxides play a vital role in biogeochemical cycles of organic pollutants.[27] MnO_2, the most prevalent form, possesses strong redox potential (E_0 = 1.23 V), enabling electron–transfer reactions with numerous organic contaminants adsorbed onto its surfaces.[28–30] The oxidation capability is further enhanced by reactive oxygen species (ROS) generated during MnO_2 redox cycling.[31–33] Among manganese oxides, δ-MnO_2 is particularly reactive due to its high surface Mn(III) (E_0 = 1.5 V) content.[30,34,35] Previous studies reported that δ-MnO_2 could also mediate the halogenation processes. For instance, δ-MnO_2 oxidizes iodide ions (E_0 = 0.54 V) into reactive iodine species, subsequently leading to the formation of iodinated organic compounds.[36–39] Kadoya *et al.* reported that δ-MnO_2 mediates the chlorination of guaiacol (a lignin model compound) to form chloroguaiacol in the presence of chloride ions.[40] This process is proposed to occur by oxidizing guaiacol into cationic intermediates, which subsequently react with chloride ions to generate the chlorinated product. Such evidence suggests that δ-MnO_2-mediated halogenation represents a potentially important abiotic pathway for the formation of PHCZs in natural environments.

We hypothesize that δ-MnO_2 can mediate the formation of PHCZs by oxidizing halide ions to reactive halogen species and by directly oxidizing carbazole to reactive intermediates that subsequently react with halide ions. To test this hypothesis, we systematically investigated δ-MnO_2-mediated formation of PHCZs under marine-related conditions. Specifically, we evaluated the effects of MnO_2 dosage and halide ion composition on PHCZ production and elucidated the underlying transformation pathways. This work advances understanding of geochemical processes contributing to natural PHCZ formation and highlights δ-MnO_2 as an abiotic driver of halogenated organic pollutant generation in marine and coastal ecosystems.

2 Materials and methods

2.1 Chemicals

The detailed information of carbazole and PHCZ congeners is listed in Table S1. 3,5-Dimethyl-1*H*-pyrazole (DMPZ, ≥99%) and 4-bromo-3,5-dimethyl-1*H*-pyrazole (BDMPZ, ≥99%) were purchased from Sigma-Aldrich (St. Louis, Missouri, USA). 4-Chloro-3,5-dimethylpyrazole (CDMPZ), 3,9′-bicarbazole (97%), 3-chloro-1,2-propanediol (3-CPD, 98%), 3-bromo-1,2-propanediol (3-BPD, 97%), and *N*-heptafluorobutyrylimidazole were purchased from Acmec Biochemical (Shanghai, China). Allyl alcohol (10 mg mL^{-1}) was purchased from BeNa Culture Collection (Beijing, China). High-performance liquid chromatography grade acetone, *n*-hexane, acetonitrile, and methyl alcohol were purchased from Tedia (Fairfield, IA, USA), while dichloromethane was sourced from Anaqua Chemicals Supply (Houston, TX, USA). *Tert*-butanol (≥99%) was purchased from Macklin (Shanghai, China). Formic acid (≥98%) was purchased from Anpel (Shanghai, China). Analytical grade sodium bromide (NaBr), sodium nitrate ($NaNO_3$), potassium permanganate ($KMnO_4$), and manganese chloride tetrahydrate ($MgCl_2 \cdot 4H_2O$) were purchased from Xilong Chemicals (Shantou, Guangdong, China). Guaranteed grade sodium chloride (NaCl), analytical grade sodium hydroxide (NaOH), and ascorbic acid were purchased from Sinopharm Chemical Reagent (Shanghai, China).

Salt solutions for the reactions were prepared by dissolving NaCl and NaBr solids in deionized water, and the pH was adjusted to 8.2 using 0.01 mol L^{-1} NaOH. Artificial seawater was prepared following the method described by Dickson and Goyet.[41] Real seawater with a salinity of 35 used in the experiments was collected from the South China Sea, China.

Manganese dioxide (δ-MnO_2) was synthesized according to Murray's method.[42] Briefly, 1.64 L of deionized water was purged with nitrogen gas (N_2) for 2 h prior to use, and 80 mL of 0.1 mol L^{-1} $KMnO_4$ and 160 mL of 0.1 mol L^{-1} NaOH solutions were added, followed by a dropwise addition of 120 mL of 0.1 mol L^{-1} $MnCl_2$ while maintaining constant nitrogen sparging. The formed δ-MnO_2 particles were collected by centrifugation and rinsed several times with deionized water until the conductivity of the supernatant matched that of deionized water. The resulting δ-MnO_2 suspensions were stored at 4 °C and diluted to appropriate concentrations prior to use. To quantify the Mn content, the δ-MnO_2 particles were dissolved using ascorbic acid and subsequently analyzed on an inductively coupled plasma mass spectrometer (NexION 2000, PerkinElmer, Shelton, CT). The zeta potential of the synthesized δ-MnO_2 was measured to be −16.6 mV at pH 7.0. A portion of the synthetic δ-MnO_2 was air-dried, and its specific surface area was determined to be 325 m^2 g^{-1} using the Brunauer–Emmett–Teller method based on N_2 adsorption on an Autosorb-iQ-MP-C automated gas sorption analyzer (Quantachrome Instruments, Boynton Beach, FL). Scanning electron microscopy and X-ray diffraction analyses indicated that the synthetic δ-MnO_2 particles consisted of amorphous, irregular aggregates (Fig. S1).

2.2 δ-MnO_2 oxidation experiment

The reactions were carried out in a 250 mL Erlenmeyer flask. First, 30 μL of 5 mmol L^{-1} carbazole (dissolved in methanol) was added to each flask. After the solvent evaporated, 30 mL of salt solution and an appropriate volume of δ-MnO_2 suspension were sequentially added. The mixture was homogenized to initiate the reaction. Triplicate samples were prepared for each treatment, and all samples were kept in the dark at 25 °C with continuous shaking at 120 rpm. At designated time intervals, triplicate samples were withdrawn, and the reaction was immediately quenched by adding an excess amount of ascorbic acid to dissolve the δ-MnO_2. Unless otherwise noted, the

reaction was carried out at 25 ± 1 °C for 24 h, with initial concentrations of 5.0 μmol L^{-1} for carbazole, 0.8 mmol L^{-1} for Br^-, and 100 μmol L^{-1} for δ-MnO_2. The pH was set at 8.2 to simulate seawater conditions.

To assess the transformation of carbazole and formation of reaction products, 30 mL of the reaction solution was collected and extracted three times each with 15 mL of fresh dichloromethane. The organic phases were combined and evaporated to dryness, and the residue was redissolved in 1 mL of acetonitrile. The final samples were filtered through a PTFE filter (0.22 μm, Jinteng, Tianjin, China) and stored at 4 °C before instrumental analysis.

To investigate the effect of δ-MnO_2 concentration, δ-MnO_2 concentrations were set at 100, 200, and 500 μmol L^{-1}. To explore the effect of halide ion concentration, Br^- concentrations were set at 0.08, 0.2, and 0.8 mmol L^{-1} and Cl^- concentrations were set at 5.4, 54.0, and 540.0 mmol L^{-1}. To assess the effect of the molar ratio of Cl^- to Br^-([Cl^-] : [Br^-]), their ratios were set at 0, 10 : 1, 100 : 1, and 500 : 1, while keeping the Br^- concentration at 0.8 mmol L^{-1}. When exploring the effect of the [Cl^-] : [Br^-] ratio, $NaNO_3$ was added to maintain a constant Na^+ concentration, eliminating the potential influence of Na^+ on MnO_2 oxidation.

2.3 Identification of reactive halogen species

The generation of reactive halogen species (RHS), including reactive chlorine species (RCS) and reactive bromine species (RBS), in the δ-MnO_2 reaction system was identified using allyl alcohol and DMPZ as chemical probes. Allyl alcohol reacts with RHS to produce 3-CPD and 3-BPD,[43,44] while DMPZ reacts with RHS to yield 4-chloro-3,5-dimethylpyrazole (CDMPZ) and BDMPZ.[45]

For the allyl alcohol probe experiments, the reaction was conducted under conditions identical to those used for carbazole oxidation, except that the carbazole substrate was replaced with 20 μL of 10 mg mL^{-1} allyl alcohol. After 24 h of reaction, 10 mL of the reaction mixture was collected, and excess Na_2SO_3 and $NaHSO_3$ were added to quench the residual RHS and dissolve the δ-MnO_2. The sample was extracted three times with 5 mL ethyl acetate, vortexing for 60 s each time. The organic phase was collected, combined, dehydrated using anhydrous Na_2SO_4, and concentrated under nitrogen blow to approximately 100 μL. The residue was reconstituted in 2 mL of acetonitrile, followed by the addition of 50 μL heptafluorobutanoyl imidazole. The mixture was stirred for 60 s and heated at 70 °C in a water bath for 30 min to derivatize 3-CPD and 3-BPD into 1,2-bis(heptafluorobutyryloxy)-3-chloropropane and 1,2-bis(heptafluorobutyryloxy)-3-bromopropane, respectively. After cooling to room temperature, the sample was diluted with 5 mL of deionized water and 2 mL of saturated NaCl solution, followed by extraction with 2 mL of *n*-hexane. The extraction was repeated twice, and the combined *n*-hexane extracts were concentrated to 1 mL under a gentle nitrogen flow. The final extract was transferred to a 2 mL vial for analysis. The analysis was carried out on a gas chromatography-mass spectrometer (GCMS-QP2010 Ultra, Shimadzu, Tokyo, Japan). The separation was achieved on a DB-5MS capillary column (50 m × 0.25 mm, 0.25 μm film thickness). The injection (1.0 μL) was in splitless mode at 250 °C, with high-purity helium (99.999%) as a carrier gas at 1.0 mL min^{-1}. The oven temperature started at 60 °C (held for 1 min), followed by heating to 120 °C at 5 °C min^{-1} (held for 3 min), then increased to 250 °C at 20 °C min^{-1} and held for 2 min. The MS was operated in electron impact mode (70 eV). Selected ions were *m*/*z* 253, 289, and 453 for 1,2-bis(heptafluorobutyryloxy)-3-chloropropane and 197, 225, and 467 for 1,2-bis(heptafluorobutyryloxy)-3-bromopropane.

For experiments employing DMPZ as the probe, the carbazole substrate was replaced with 30 μL of 100 mmol L^{-1} DMPZ. Triplicate samples were prepared for each treatment. At designated time intervals, triplicate samples were withdrawn and excess ascorbic acid solution was added to quench the reaction by dissolving δ-MnO_2. The samples were then filtered through a 0.22 μm PVDF membrane filter (Jinteng, Tianjin, China) and analyzed directly by LC-MS/MS. The derivatized BDMPZ and CDMPZ were analyzed on a liquid chromatography-triple quadrupole mass spectrometer (Agilent 1290 Infinity LC-6490 MS/MS) equipped with an electrospray ionization (ESI) source (Agilent, Palo Alto, CA, USA). The MS was operated in positive ion (ESI+) mode with multiple reaction monitoring. For the detection of BDMPZ, precursor ion *m*/*z* 175 and product ions *m*/*z* 95/54 were selected. The quantitative ion was *m*/*z* 95. The collision energies were optimized to be 30 eV for *m*/*z* 95 and 40 eV for *m*/*z* 54. For the detection of CDMPZ, precursor ion *m*/*z* 131 and product ions *m*/*z* 54/62.8 were selected. The quantitative ion was *m*/*z* 54. The collision energies were optimized to be 25 eV for *m*/*z* 54 and 20 eV for *m*/*z* 62.8. Other MS parameters followed those of Zhang and Lin.[22] The mobile phase consisted of ultrapure water (A) and acetonitrile containing 0.1% formic acid (B), with a flow rate of 0.20 mL min^{-1} and an injection volume of 5 μL. To achieve optimal separation, the gradient elution program was 0–2 min, 5% B; 2–4 min, 5–30% B; 4–7 min, hold at 30% B; 7–9 min, 30–5% B; and 7–12 min, hold at 5% B to restore the initial conditions. To prevent salt contamination, the eluent was directed to waste for the first 5 min before switching to MS detection.

2.4 Analysis of carbazole and reaction products

The concentrations of carbazole and PHCZs were determined using LC-MS/MS. The mobile phase comprised water (A) and acetonitrile (B) at a flow rate of 0.25 mL min^{-1}. The gradient elution program was 0–1 min, hold at 55% B; 1–8 min, a linear increase to 80% B; 8–15 min, hold at 90% B; 15–17 min, hold at 90% B; 17–17.1 min, return to 55% B; 17.01–20 min, equilibrate at 55% B. The MS was operated in negative ion (ESI−) mode with multiple reaction monitoring for the quantification of carbazole and PHCZs. The MS/MS parameters followed those of Zhou *et al.*[46]

For unknown reaction product analysis, LC-MS/MS was operated in full scan and product ion scan modes. In full scan mode, the *m*/*z* range was set from 60 to 800. In the product ion scans, the *m*/*z* scan range was set from 60 to (M + 20) (M denotes

the molecular weight) and collision energies were varied from 5 to 70 eV, depending on the fragment structure. Potential products were screened from full scan results, and suspected compounds were confirmed by comparing retention times and fragmentation patterns with those of authentic standards.

3 Results and discussion

3.1 δ-MnO_2-mediated transformation of carbazole into PHCZs and other products

The results showed that δ-MnO_2 catalyzed the transformation of carbazole into PHCZs in solutions containing various concentrations of halide ions (Fig. 1). In the presence of Br^- and Cl^-, the reaction produced both mono- and di-halogenated carbazoles. Specifically, in the solution containing 0.8 mmol L^{-1} Br^- and 0.54 mol L^{-1} Cl^-, three PHCZ congeners were detected, including 3-BCZ (4.8×10^{-1} μg L^{-1}), 36-BCZ (3.0×10^{-2} μg L^{-1}), and 3-CCZ (1.4×10^{-1} μg L^{-1}) (Fig. 1). Notably, despite the Br^- concentration being much lower than that of Cl^-, brominated carbazoles dominated the product species, indicating that Br^- is substantially more reactive than Cl^- in the reaction system. This higher reactivity can also explain the detection of 3-BCZ in the reaction with 0.54 mol L^{-1} Cl^- alone, likely due to trace Br^- impurities.

In artificial seawater, only 3-BCZ (1.1×10^{-2} μg L^{-1}) was detected (Fig. 1), an order of magnitude lower than that in the mixed-halide system with comparable halide concentrations. Similarly, a higher concentration of 3-BCZ (0.3×10^{-1} μg L^{-1}) was formed in natural seawater. This discrepancy suggests that other components in artificial and natural seawater, particularly high concentrations of metal cations, may suppress δ-MnO_2-mediated PHCZ formation. Previous studies have shown that high levels of Ca^{2+} and Mg^{2+} can reduce the reactivity of δ-MnO_2 in two ways: (i) by adsorbing onto the negatively charged δ-MnO_2 surface (the point of zero charge $pH_{pzc} = 2.4$), altering surface structure, reducing colloidal stability, and inducing precipitation[29,47,48] and (ii) by occupying surface reactive sites, thereby blocking access for organic substrates.[49,50] Both effects can inhibit the δ-MnO_2-mediated transformation of carbazole into PHCZs. The differences observed between artificial and natural seawater may also arise from variations in halide ion concentrations and the presence of natural organic matter, which influence the complex transformation process among carbazole, halide ions and MnO_2.

The concentration of δ-MnO_2 significantly influenced the formation of PHCZs (Fig. S2). As the δ-MnO_2 concentration increased from 100 μmol L^{-1} to 500 μmol L^{-1}, the final production of 3-BCZ and 36-BCZ gradually decreased. This decline is likely due to the further oxidation of 3-BCZ and 36-BCZ through oxidative reactions between δ-MnO_2 and these products, as supported by the results shown in Fig. S3. Like carbazole, 3-BCZ and 36-BCZ may first adsorb onto the δ-MnO_2 active sites, followed by electron transfer. Higher δ-MnO_2 concentrations increase the number of reactive sites, which enhances the oxidative breakdown of both carbazole and PHCZ products, ultimately reducing the final PHCZ yield.

Fig. S4A illustrates the strong oxidizing ability of δ-MnO_2 toward carbazole. In the reaction system containing δ-MnO_2, carbazole removal was nearly complete, accompanied by the release of Mn^{2+}, the reductive product of δ-MnO_2. This can be attributed to two factors: (i) carbazole's redox potential (0.93 V) is lower than that of δ-MnO_2 (1.23 V),[51] making oxidation thermodynamically favorable and (ii) alternative transformation pathways, such as oxidative coupling, may occur.[29,52] Evidence for oxidative coupling was obtained *via* mass spectrometry, revealing a distinct chromatographic peak at *m/z* 330.8,

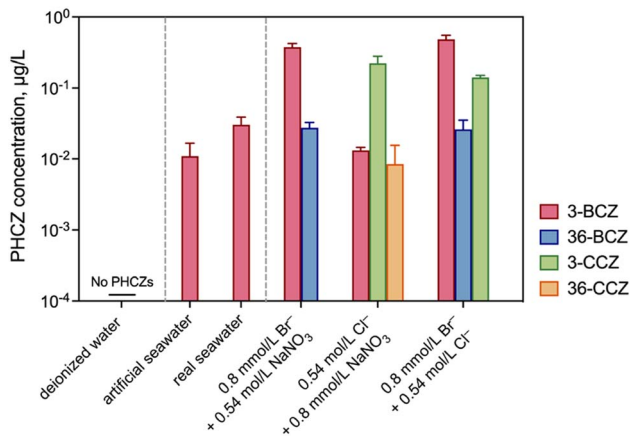

Fig. 1 δ-MnO_2-mediated transformation of carbazole into PHCZs in different solutions. The initial concentrations of carbazole and δ-MnO_2 were 5 μmol L^{-1} and 100 μmol L^{-1}, respectively. The pH of the solution was adjusted to 8.2 and the reaction was conducted at 25 °C for 24 h.

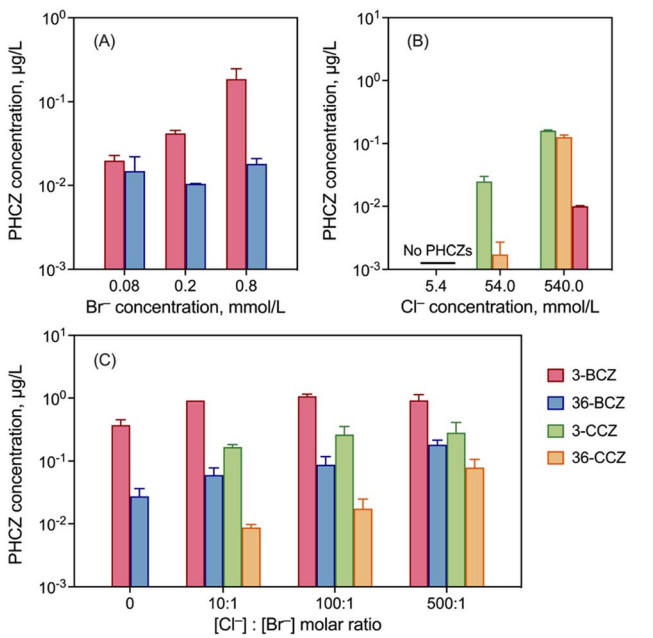

Fig. 2 Effect of Br^- concentration (A), Cl^- concentration (B), and Cl^-/Br^- ratio (C) on PHCZ production. The initial concentrations of carbazole and δ-MnO_2 were 5 μmol L^{-1} and 100 μmol L^{-1}, respectively. The initial concentration of Br^- was 0.8 mmol L^{-1} in panel (C), and $NaNO_3$ was added to maintain a constant Na^+ concentration to eliminate the potential influence of Na^+ on MnO_2 oxidation. The pH of the solution was adjusted to 8.2 and the reaction was conducted at 25 °C for 24 h.

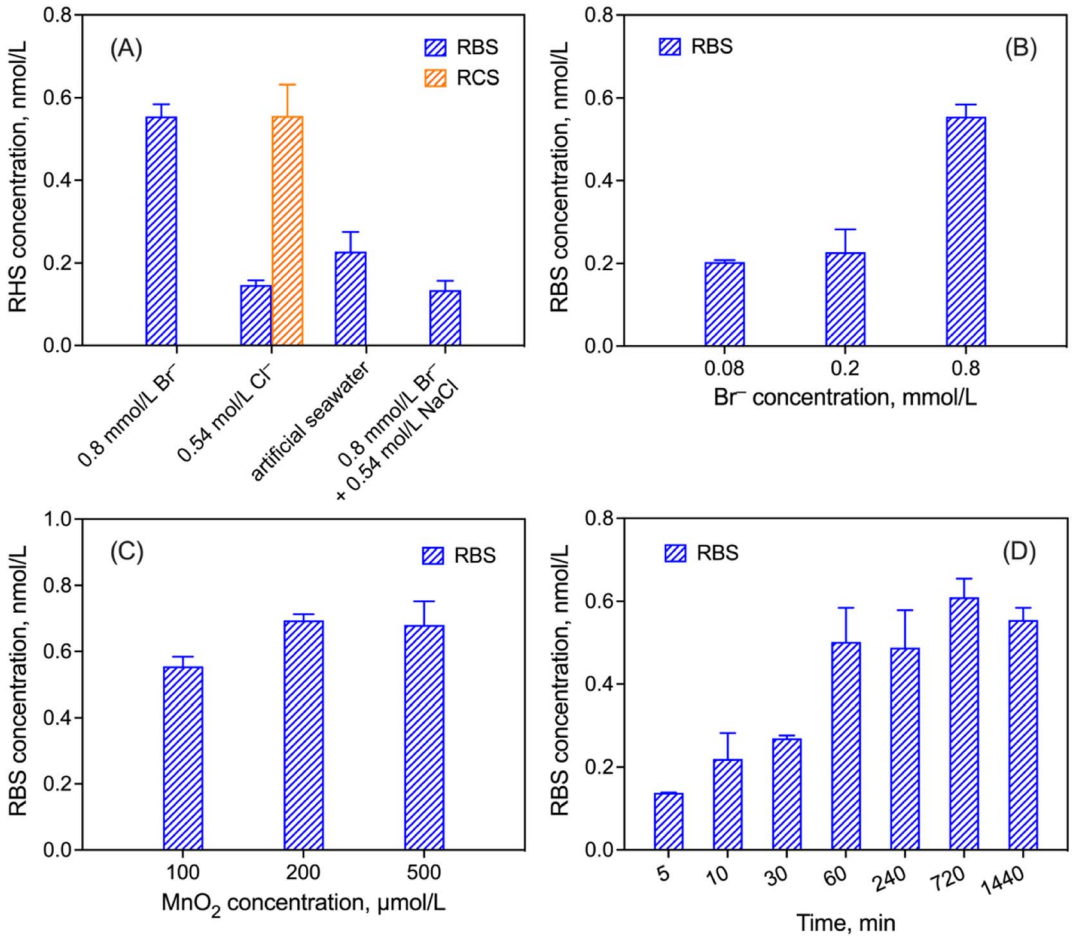

Fig. 3 Effect of reaction solutions (A), Br^- concentration (B), MnO_2 concentration (C), and reaction time (D) on the generation of reactive halogen species (RHS). Unless specified, the reaction solution contained 0.8 mmol L^{-1} NaBr and 100 μmol L^{-1} δ-MnO_2 and the reaction time was 24 h. The solution pH was adjusted to 8.2.

corresponding to a carbazole dimer (Fig. S4B). The major fragment ion at *m*/*z* 165.9 corresponded to the carbazole monomer. Based on retention time and mass spectral comparison with those of an authentic standard, the unknown compound was identified as 3,9′-bicarbazole (Fig. S4C).

3.2 Effect of halide ions

Halide ions act as halogen donors for the halogenation process, directly influencing PHCZ yield. As shown in Fig. 2A, increasing Br^- concentration from 0.08 mmol L^{-1} to 0.8 mmol L^{-1} led to nearly a tenfold increase in 3-BCZ. Under conditions containing 5.4 mmol L^{-1} of Cl^-, no chlorinated carbazoles were detected. However, when the Cl^- concentration was elevated from 54.0 mmol L^{-1} to 540 mmol L^{-1}, the concentrations of 3-CCZ and 36-CCZ rose from 2.5×10^{-2} μg L^{-1} and 1.7×10^{-3} μg L^{-1} to 1.6×10^{-1} μg L^{-1} and 1.3×10^{-1} μg L^{-1}, respectively (Fig. 2B). These results clearly show that δ-MnO_2-mediated PHCZ formation is halide concentration-dependent, with higher Br^- and Cl^- levels promoting increased yields of their respective halogenated carbazoles.

Given that Br^- and Cl^- often coexist in marine environments, we further examined the effect of their molar ratio on PHCZ formation. The molar ratios of Cl^- to Br^- ($[Cl^-]:[Br^-]$) were varied at 0, 10 : 1, 100 : 1, and 500 : 1, while keeping the Br^- concentration at 0.8 mmol L^{-1}. The results demonstrated that the increasing proportion of Cl^- enhanced the formation of both chlorinated and brominated carbazoles (Fig. 2C). This effect may be explained by two factors: (i) higher Cl^- availability facilitates its adsorption to reactive δ-MnO_2 sites, directly promoting 3-CCZ and 36-CCZ formation and (ii) greater Cl^- surface occupation may partially suppress further oxidative degradation of halogenated carbazoles by δ-MnO_2, thereby improving their final yield.

3.3 Production of RHS

To further probe how halide ions influence PHCZ formation, the generation of RHS in the reaction system was investigated. RHS are key intermediates in the formation of halogenated organic compounds; therefore, their detection was essential for understanding the reaction mechanism. Phenolic chemical probes commonly used for RHS detection (*e.g.*, 2,6-dichlorophenol) can be readily oxidized by δ-MnO_2, leading to potential interference. In contrast, allyl alcohol and DMPZ are inert to δ-MnO_2, making them suitable probes in this study.

Since the allyl alcohol derivatives 3-CPD and 3-BPD can undergo further reactions with allyl alcohol,[43,44] allyl alcohol was used only for qualitative identification of RHS. DMPZ, however, reacts stoichiometrically (1 : 1 molar ratio) with RCS and RBS to form CDMPZ and BDMPZ, respectively,[45] and was therefore used for quantitative analysis.

The results consistently confirmed RHS generation in solutions containing either Cl^- or Br^- (Fig. 3 and S5). In the reaction system with 0.54 mol L^{-1} Cl^-, 0.55 nmol L^{-1} RCS and 0.15 nmol L^{-1} RBS were detected, with the formation of RBS primarily attributed to trace bromide Br^- impurities in the NaCl reagent. In both the mixed-halide system and the artificial seawater system, only RBS was detected while no RCS was observed. This result can be explained by the fact that both high Br^- concentrations and the generated RBS can convert RCS into other RBS, such as HOBr and BrOCl, as shown in eqn (1) and (2).[53,54]

$$HOCl + Br^- \rightleftharpoons HOBr + Cl^- \quad (1)$$

$$HOCl + HOBr \rightleftharpoons BrOCl + H_2O \quad (2)$$

Both the Br^- concentration and δ-MnO_2 concentration significantly influenced RBS generation (Fig. 3B and C). Increasing the Br^- concentration from 0.08 mmol L^{-1} to 0.8 mmol L^{-1} increased RBS yield from 0.2 nmol L^{-1} to 0.56 nmol L^{-1}, likely due to more Br^- binding to reactive δ-MnO_2 sites and promoting MnO_2-mediated RBS formation. Increasing the δ-MnO_2 concentration from 100 μmol L^{-1} to 200 μmol L^{-1} raised RBS production from 0.56 nmol L^{-1} to 0.69 nmol L; however, further increasing δ-MnO_2 to 500 μmol L^{-1} did not significantly enhance RBS generation. This result suggests that once δ-MnO_2 reaches an excess level, Br^- availability becomes the limiting factor for further RBS production.

The production of RBS gradually increased with reaction time before eventually reaching a plateau (Fig. 3D). This trend might be attributed to the continuous release of Mn^{2+}, the reduction product of δ-MnO_2, into the reaction system as the reaction progresses.[29,55,56] On the one hand, Mn^{2+} readily adsorbs on the δ-MnO_2 surface, occupying reactive sites that would otherwise be available for Br^- binding. The adsorption of Mn^{2+} and its inhibitory effect on the oxidative capacity of δ-MnO_2 have been extensively documented in studies focusing on δ-MnO_2-catalyzed oxidation of hydroquinone, phenols, and anilines.[30,55,57]

$$MnO_2(s) + 4H^+ + 2e^- \rightarrow Mn^{2+}(aq) + 2H_2O \quad (3)$$

The Nernst equation

$$E_h = E_0 + 0.0296 \lg \frac{[MnO_2][H^+]^4}{[Mn^{2+}]} \quad (4)$$

predicts that the accumulation of Mn^{2+} would lower the redox potential of δ-MnO_2. Together, Mn^{2+} surface adsorption and the decrease in δ-MnO_2 redox potential reduce its ability to generate RHS, ultimately leading to the stabilization of RBS production over time.

The generation of RBS may occur *via* two potential pathways. First, the redox potentials of δ-MnO_2 (E_0 = 1.23 V) and the Mn(III) species (E_0 = 1.50 V) within δ-MnO_2 are higher than that of Br^- (E_0 = 1.09 V), enabling direct oxidation of Br^- to Br_2. Second, previous studies have demonstrated that when molecular oxygen (O_2) adsorbs vertically onto the surface oxygen vacancies in MnO_2 and is bound to adjacent Mn(III) atoms, single-electron transfer from Mn(III) to O_2 occurs, leading to sustained production of $O_2^{\bullet-}$ [31,32,58] This superoxide can be converted to other reactive oxygen species (ROS), such as $^{\bullet}OH$, through a series of radical reactions (eqn (5)–(7)). Wang *et al.* detected $^{\bullet}OH$ generation in MnO_2 with different crystallinities and confirmed significant contribution of $^{\bullet}OH$ to the mineralization of dissolved organic matter.[33] Given that $^{\bullet}OH$ is the most powerful oxidative ROS (E_0 = 2.8 V), it can further oxidize Br^-, thereby facilitating the production of RBS.

$$2O_2^{\bullet-} + 2H^+ \rightarrow H_2O_2 + O_2 \quad (5)$$

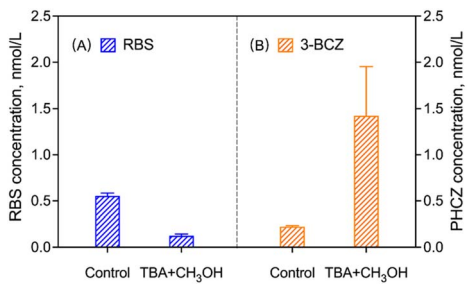

Fig. 4 Effect of *tert*-butanol (TBA) and methanol on the generation of RBS (A) and PHCZs (B). Conditions in panel (A): the reaction was carried out in 0.8 mmol L^{-1} NaBr solution with pH adjusted to 8.2. The initial concentrations of DMPZ and δ-MnO_2 were both 100 μmol L^{-1}. The initial concentrations of TBA and CH_3OH were both 200 mmol L^{-1} in experimental groups. No TBA or CH_3OH was added in control groups. The reaction time was 24 h. Conditions in panel (B): after 24 h of reaction in the system shown in panel (A), 5 μmol L^{-1} of carbazole was added, and the mixture was allowed to react for an additional 24 h.

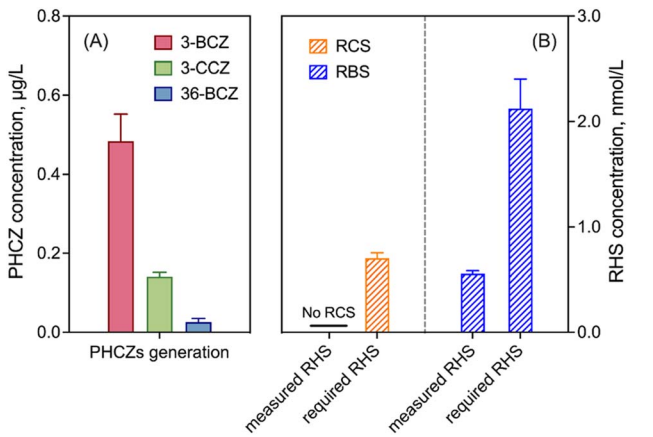

Fig. 5 The generation of PHCZs (A), RHS, and the required amount of RHS to generate PHCZs (B) in the mixed halide solution. The initial concentration of carbazole and δ-MnO_2 was 5 μmol L^{-1} and 100 μmol L^{-1}, respectively with a reaction time of 24 h. For the investigation of RHS production, the substrate carbazole was replaced with 100 μmol L^{-1} of DMPZ.

$$O_2^{\bullet-} + H_2O_2 \rightarrow O_2 + {}^{\bullet}OH + OH^- \quad (6)$$

$$H_2O_2 + Mn(III) \rightarrow Mn(IV) + {}^{\bullet}OH + OH^- \quad (7)$$

To investigate whether ˙OH participates in RBS generation, 200 mmol L^{-1} *tert*-butanol and 200 mmol L^{-1} methanol were added into the reaction systems as ˙OH scavengers. The addition of these scavengers significantly reduced RBS production from 0.56 nmol L^{-1} to 0.12 nmol L^{-1}, while simultaneously increasing the yield of 3-BCZ (Fig. 4). This pronounced reduction of RBS confirms that RBS formation predominantly depended on ROS, particularly ˙OH. The residual RBS detected in the system likely originated from the direct oxidation of Br^- by MnO_2 and Mn(III). The higher 3-BCZ yields likely resulted from the inhibition of its further oxidative degradation due to ˙OH scavenging.

Since RCS was not detected in real seawater, it is unlikely that RCS form under typical environmental conditions. Thus, the formation mechanism of RCS is not discussed in detail. Nonetheless, trace amounts of RCS could potentially be generated through pathways analogous to those of RBS formation, likely mediated by Mn(III) and ROS-driven oxidation, considering the relatively high redox potential of Cl_2/Cl^- (1.36 V), which makes its direct oxidation by δ-MnO_2 less favorable than that of Br^-.

3.4 Potential PHCZ formation pathways

The potential pathways for PHCZ formation are outlined in Fig. 6. In brief, δ-MnO_2-mediated transformation of carbazole into PHCZs likely occurs *via* two distinct pathways: (i) electrophilic substitution involving δ-MnO_2-generated RHS (pathway I) and (ii) nucleophilic addition of halide ions to the carbazole cation formed through δ-MnO_2 oxidation (pathway II).

In the electrophilic substitution pathway, δ-MnO_2 generates RHS, such as Br_2, HOBr, and their chlorinated analogs, which

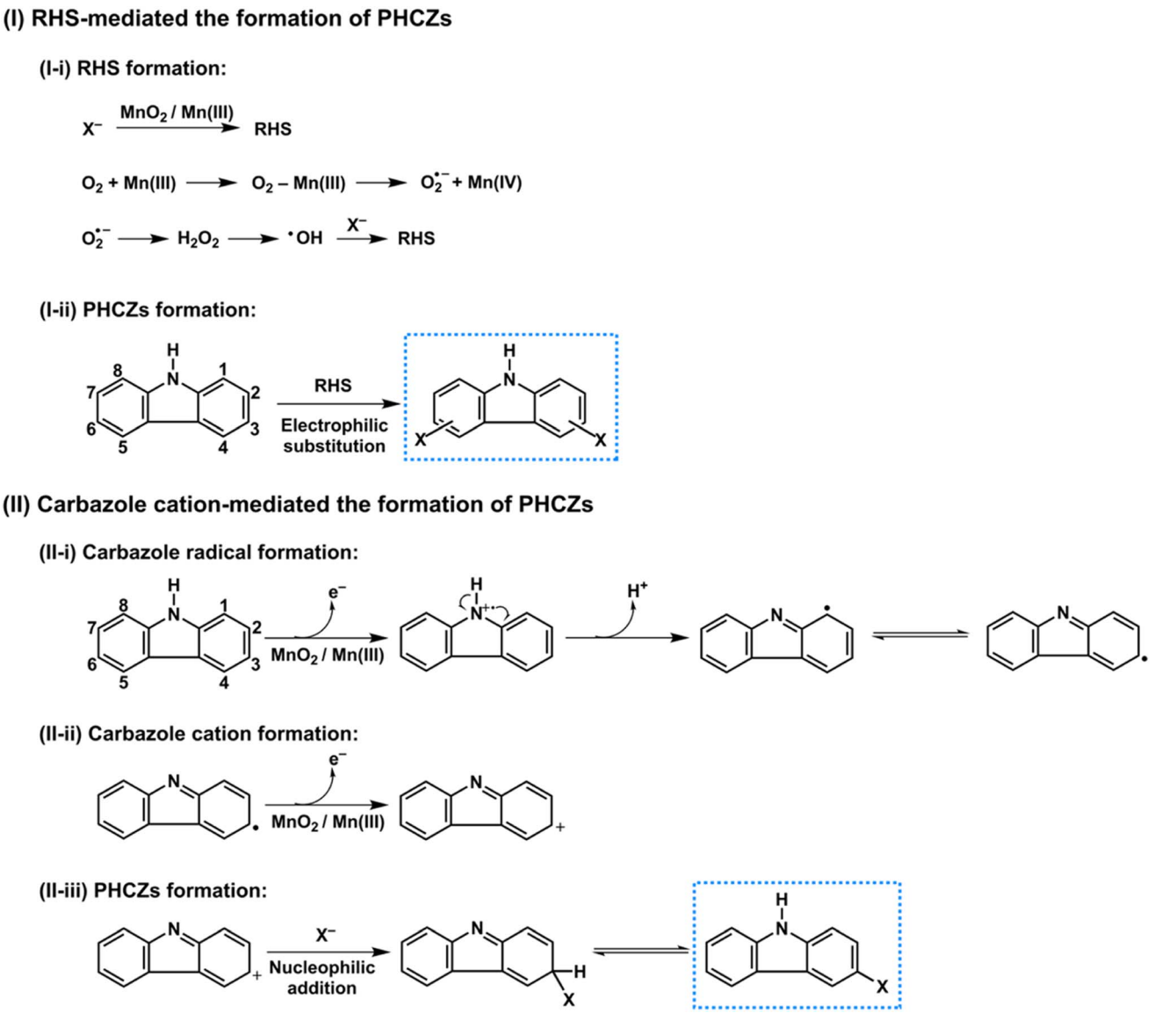

Fig. 6 Proposed reaction pathways for MnO_2-mediated transformation of carbazole into PHCZs.

subsequently attack the electron-rich carbazole ring. In aqueous systems, δ-MnO_2 oxidizes halide ions (*e.g.*, Br^- and Cl^-) either directly or *via* intermediate ROS, producing RHS with strong electrophilic reactivity. Carbazole, with its high electron density at the C-3 position due to resonance effects from the nitrogen atom, is particularly susceptible to electrophilic attack.[59] The RHS species preferentially substitute at this C-3 position, forming halogenated carbazole derivatives such as 3-BCZ and 3-CCZ. This pathway is supported by the detection of PHCZs in δ-MnO_2/halide systems, even in the absence of other known halogenating agents, highlighting the important role of δ-MnO_2-generated RHS in initiating halogenation.

Although electrophilic substitution by δ-MnO_2-generated RHS represents a key pathway for PHCZ formation, additional mechanisms are likely involved. Two observations support this: (i) in the presence of $^{\bullet}OH$ scavengers, the yield of 3-BCZ exceeded the measured RBS concentration (Fig. 4) and (ii) 3-CCZ was detected despite the absence of measurable RCS in a mixed-halide solution containing 0.8 mmol L^{-1} Br^- and 0.54 mol L^{-1} Cl^-, with the RBS concentration theoretically required for the detected brominated carbazoles being much higher than the measured value (Fig. 5). Similarly, a previous study demonstrated that δ-MnO_2 can oxidize guaiacol to a phenoxy radical, which undergoes further one-electron oxidation to form a phenoxenium cation. This cation reacts with chloride or bromide to form chloroguaiacol and bromoguaiacol.[40] Given carbazole's electron-rich aromatic structure and relatively low redox potential, it is prone to electron transfer with δ-MnO_2, making a similar pathway plausible. We propose that direct δ-MnO_2-mediated transformation of carbazole into PHCZs involves the following steps: (i) radical formation: the nitrogen atom's lone electron pair facilitates electron transfer to δ-MnO_2, generating a carbazole radical. The unpaired electron delocalizes within the conjugated system, localizing at the C-3 position; (ii) cation formation: the carbazole radical undergoes further oxidation by δ-MnO_2 or Mn(III) to yield a carbazole cation; (iii) nucleophilic addition: halide ions attack the carbazole cation at C-3, followed by isomerization to form 3-BCZ or 3-CCZ.

4 Conclusions

This study demonstrates that δ-MnO_2 can mediate the transformation of carbazole into PHCZs under marine-related conditions. The formation of PHCZs likely proceeds through two concurrent pathways: (i) electrophilic substitution, where carbazole reacts with reactive halogen species generated by the oxidation of halide ions by δ-MnO_2, and (ii) nucleophilic addition, where halide ions attack carbazole cations produced *via* δ-MnO_2-induced oxidation. Elevated halide ion concentrations, particularly Br^-, significantly enhance PHCZ formation. Given the widespread presence of halide ions, manganese oxides, and carbazole in marine environments, these findings suggest that δ-MnO_2-mediated halogenation could be an important natural pathway for PHCZ formation. This study provides new insights into the abiotic processes contributing to the environmental load of PHCZs and highlights δ-MnO_2 as a key geochemical driver of halogenated organic compound formation in coastal and marine ecosystems.

Conflicts of interest

The authors declare that they have no known competing financial interests or personal relationships that could have appeared to influence the work reported in this paper.

Data availability

The data supporting this article have been included as part of the supplementary information (SI). Supplementary information: Table S1 and Fig. S1–S5. See DOI: https://doi.org/10.1039/d6em00064a.

Acknowledgements

This work was financially supported by the National Natural Science Foundation of China (22276156).

References

1 J. Guo, D. Chen, D. Potter, K. J. Rockne, N. C. Sturchio, J. P. Giesy, *et al.*, Polyhalogenated carbazoles in sediments of lake Michigan: A new discovery, *Environ. Sci. Technol.*, 2014, **48**(21), 12807–12815.
2 J. Guo, Z. Li, P. Ranasinghe, S. Bonina, S. Hosseini, M. B. Corcoran, *et al.*, Spatial and temporal trends of polyhalogenated carbazoles in sediments of upper Great Lakes: Insights into their origin, *Environ. Sci. Technol.*, 2017, **51**(1), 89–97.
3 W. Zhou, W. Chen, P. Li, Z. Gu, J. Peng and K. Lin, Occurrence and distribution of polyhalogenated carbazoles (PHCs) in sediments from the northern South China Sea, *Sci. Total Environ.*, 2021, **753**, 142072.
4 A. Li, S. Zhou, H. He, J. Guo, K. J. Rockne, N. C. Sturchio, *et al.*, Polyhalogenated carbazoles in sediments of lower Laurentian Great Lakes and regional perspectives, *ACS ES&T Water*, 2022, **2**(9), 1544–1554.
5 S. Hu, L. Jiang, L. Jiang, L. Tang, A. U. K. Wickrama Arachchige, H. Yu, *et al.*, Spatial distribution characteristics of carbazole and polyhalogenated carbazoles in water column and sediments in the open Western Pacific Ocean, *J. Hazard. Mater.*, 2024, **469**, 133956.
6 Y. Zhou, G. Zhu, M. Li, J. Liu, Z. Li, J. Sun, *et al.*, Method development for analyzing ultratrace polyhalogenated carbazoles in soil and sediment, *Ecotoxicol. Environ. Saf.*, 2019, **182**, 109470.
7 M. Liu, L. Huang, X. Li, F. Liu, W. Zhang, Z. Wang, *et al.*, Occurrence and distribution of polyhalogenated carbazoles in eastern Tibetan Plateau soils along the slope of Mt. Qionglai, *Chemosphere*, 2022, **298**, 134200.
8 Q. Zou, Q. Zhang, R. Yang, Y. Li, Z. Pei, M. Liu, *et al.*, Non-negligible polyhalogenated carbazoles in arctic soils and sediments: Occurrence, target and suspect screening, and

potential sources, *Environ. Sci. Technol.*, 2024, **58**(52), 23169–23179.
9 H. Fromme, W. Mi, T. Lahrz, M. Kraft, B. Aschenbrenner, B. Bruessow, *et al.*, Occurrence of carbazoles in dust and air samples from different locations in Germany, *Sci. Total Environ.*, 2018, **610–611**, 412–418.
10 H. Zhou, X. Dong, N. Zhao, M. Zhao and H. Jin, Polyhalogenated carbazoles in indoor dust from Hangzhou, China, *Sci. Total Environ.*, 2023, **859**, 159971.
11 H. Hu, M. Zhao, Y. Guo, Y. Zhou, T. Li, W. Zhu, *et al.*, Occurrence, bioaccumulation and potential risk of polyhalogenated carbazoles in marine organisms from the East China Sea, *Sci. Total Environ.*, 2022, **807**, 150643.
12 M. Zhang, P. Li, Q. Wang, L. Huang and K. Lin, Production of polyhalogenated carbazoles in marine red alga Corallina officinalis: A possible natural source, *Environ. Sci. Technol.*, 2023, **57**(16), 6673–6681.
13 Y. Wu, H. Tan, R. Sutton and D. Chen, From sediment to top predators: Broad exposure of polyhalogenated carbazoles in San Francisco Bay (U.S.A.), *Environ. Sci. Technol.*, 2017, **51**(4), 2038–2046.
14 J. Mumbo, B. Henkelmann, A. Abdelaziz, G. Pfister, N. Nguyen, R. Schroll, *et al.*, Persistence and dioxin-like toxicity of carbazole and chlorocarbazoles in soil, *Environ. Sci. Pollut. Res.*, 2015, **22**(2), 1344–1356.
15 M. Fang, J. Guo, D. Chen, A. Li, D. E. Hinton and W. Dong, Halogenated carbazoles induce cardiotoxicity in developing zebrafish (Danio rerio) embryos, *Environ. Toxicol. Chem.*, 2016, **35**(10), 2523–2529.
16 C. Ji, L. Yan, Y. Chen, S. Yue, Q. Dong, J. Chen, *et al.*, Evaluation of the developmental toxicity of 2,7-dibromocarbazole to zebrafish based on transcriptomics assay, *J. Hazard. Mater.*, 2019, **368**, 514–522.
17 M. Dong, J. Wang, Y. Liu, Q. He, H. Sun, Z. Xu, *et al.*, 3-bromocarbazole-induced developmental neurotoxicity and effect mechanisms in zebrafish, *ACS ES&T Water*, 2023, **3**(8), 2471–2480.
18 S. Yue, T. Zhang, Q. Shen, Q. Song, C. Ji, Y. Chen, *et al.*, Assessment of endocrine-disrupting effects of emerging polyhalogenated carbazoles (PHCZs): In vitro, in silico, and in vivo evidence, *Environ. Int.*, 2020, **140**, 105729.
19 X. Wang, M. Hu, M. Li, F. Huan, R. Gao and J. Wang, Effects of exposure to 3,6-DBCZ on neurotoxicity and AhR pathway during early life stages of zebrafish (Danio rerio), *Ecotoxicol. Environ. Saf.*, 2024, **270**, 115892.
20 G. Wang, J. Yang, S. Gao, H. Hou, K. Xiao, J. Hu, *et al.*, New insight into the formation of polyhalogenated carbazoles: Aqueous chlorination of residual carbazole under bromide condition in drinking water, *Water Res.*, 2019, **159**, 252–261.
21 G. Wang, T. Jiang, S. Li, H. Hou, K. Xiao, J. Hu, *et al.*, Occurrence and exposure risk evaluation of polyhalogenated carbazoles (PHCZs) in drinking water, *Sci. Total Environ.*, 2021, **750**, 141615.
22 M. Zhang and K. Lin, Insight into the formation of polyhalogenated carbazoles during seawater chlorination, *Water Res.*, 2023, **238**, 120009.
23 Y. Sun, L. Yang, M. Zheng, R. Weber, J. Falandysz, G. Lammel, *et al.*, Industrial source identification of polyhalogenated carbazoles and preliminary assessment of their global emissions, *Nat. Commun.*, 2023, **14**(1), 3740.
24 M. Zhang and K. Lin, Unintended polyhalogenated carbazole production during advanced oxidation of coking wastewater, *J. Hazard. Mater.*, 2024, **473**, 134649.
25 L. Zhu and R. A. Hites, Identification of brominated carbazoles in sediment cores from Lake Michigan, *Environ. Sci. Technol.*, 2005, **39**(24), 9446–9451.
26 Y. Chen, K. Lin, D. Chen, K. Wang, W. Zhou, Y. Wu, *et al.*, Formation of environmentally relevant polyhalogenated carbazoles from chloroperoxidase-catalyzed halogenation of carbazole, *Environ. Pollut.*, 2018, **232**, 264–273.
27 W. G. Sunda, S. A. Huntsman and G. R. Harvey, Photoreduction of manganese oxides in seawater and its geochemical and biological implications, *Nature*, 1983, **301**, 234–236.
28 S. Laha and R. G. Luthy, Oxidation of aniline and other primary aromatic amines by manganese dioxide, *Environ. Sci. Technol.*, 1990, **24**(3), 363–373.
29 K. Lin, C. Yan and J. Gan, Production of hydroxylated polybrominated diphenyl ethers (oh-pbdes) from bromophenols by manganese dioxide, *Environ. Sci. Technol.*, 2014, **48**(1), 263–271.
30 C. K. Remucal and M. Ginder-Vogel, A critical review of the reactivity of manganese oxides with organic contaminants, *Environ. Sci.: Processes Impacts*, 2014, **16**(6), 1247–1266.
31 Z. Wang, H. Jia, T. Zheng, Y. Dai, C. Zhang, X. Guo, *et al.*, Promoted catalytic transformation of polycyclic aromatic hydrocarbons by MnO_2 polymorphs: Synergistic effects of Mn^{3+} and oxygen vacancies, *Appl. Catal. B Environ.*, 2020, **272**, 119030.
32 S. Zhang, J. Lv, R. Han and S. Zhang, Superoxide radical mediates the transformation of tetrabromobisphenol A by manganese oxides, *Colloids Surf., A*, 2022, **651**, 129807.
33 Z. Wang, H. Zhao, Z. Shi, H. Zhao, S. Chen, Z. Chen, *et al.*, Manganese dioxides induce the transformation and protection of dissolved organic matter simultaneously: A significance of crystallinity, *Environ. Sci. Technol.*, 2025, **59**(2), 1222–1231.
34 P. S. Nico and R. J. Zasoski, Mn(III) center availability as a rate controlling factor in the oxidation of phenol and sulfide on δ-MnO_2, *Environ. Sci. Technol.*, 2001, **35**(16), 3338–3343.
35 S. Yang, N. Shobnam, Y. Sun, F. E. Löffler and J. Im, The relative contributions of Mn(III) and Mn(IV) in manganese dioxide polymorphs to bisphenol A degradation, *J. Hazard. Mater.*, 2024, **461**, 132596.
36 P. M. Fox, J. A. Davis and G. W. Luther, The kinetics of iodide oxidation by the manganese oxide mineral birnessite, *Geochim. Cosmochim. Acta*, 2009, **73**(10), 2850–2861.
37 S. Allard and H. Gallard, Abiotic formation of methyl iodide on synthetic birnessite: A mechanistic study, *Sci. Total Environ.*, 2013, **463–464**, 169–175.
38 J. Li, S. Y. Pang, Y. Zhou, S. Sun, L. Wang, Z. Wang, *et al.*, Transformation of bisphenol AF and bisphenol S by

manganese dioxide and effect of iodide, *Water Res.*, 2018, **143**, 47–55.

39 J. Du, K. Kim, S. Son, D. Pan, S. Kim and W. Choi, MnO_2-induced oxidation of iodide in frozen solution, *Environ. Sci. Technol.*, 2023, **57**(13), 5317–5326.

40 W. M. Kadoya, C. L. Madeira, C. Hoppe-Jones, T. Solsten, S. A. Snyder, R. A. Root, *et al.*, The role of manganese dioxide in the natural formation of organochlorines, *ACS ES&T Water*, 2021, **1**(12), 2523–2530.

41 A. G. Dickson and C. Goyet *Handbook of Methods for the Analysis of the Various Parameters of the Carbon Dioxide System in Sea Water*, Oak Ridge National Lab, TN, USA. 2nd edn, 1994.

42 J. W. Murray, The surface chemistry of hydrous manganese dioxide, *J. Colloid Interface Sci.*, 1974, **46**(3), 357–371.

43 C. Anastasio and B. M. Matthew, A chemical probe technique for the determination of reactive halogen species in aqueous solution: Part 2—chloride solutions and mixed bromide/chloride solutions, *Atmos. Chem. Phys.*, 2006, **6**(9), 2439–2451.

44 B. M. Matthew and C. Anastasio, A chemical probe technique for the determination of reactive halogen species in aqueous solution: Part 1—bromide solutions, *Atmos. Chem. Phys.*, 2006, **6**(9), 2423–2437.

45 J. D. Méndez-Díaz, K. K. Shimabuku, J. Ma, Z. O. Enumah, J. J. Pignatello, W. A. Mitch, *et al.*, Sunlight-driven photochemical halogenation of dissolved organic matter in seawater: A natural abiotic source of organobromine and organoiodine, *Environ. Sci. Technol.*, 2014, **48**(13), 7418–7427.

46 W. Zhou, X. Huang and K. Lin, Analysis of polyhalogenated carbazoles in sediment using liquid chromatography–tandem mass spectrometry, *Ecotoxicol. Environ. Saf.*, 2019, **170**, 148–155.

47 H. S. Posselt, F. J. Anderson and W. J. Weber, Cation sorption on colloidal hydrous manganese dioxide, *Environ. Sci. Technol.*, 1968, **2**(12), 1087–1093.

48 K. Lin, W. Liu and J. Gan, Oxidative removal of bisphenol a by manganese dioxide: Efficacy, products, and pathways, *Environ. Sci. Technol.*, 2009, **43**(10), 3860–3864.

49 K. A. Barrett and M. B. McBride, Oxidative degradation of glyphosate and aminomethylphosphonate by manganese oxide, *Environ. Sci. Technol.*, 2005, **39**(23), 9223–9228.

50 L. Xu, C. Xu, M. Zhao, Y. Qiu and G. D. Sheng, Oxidative removal of aqueous steroid estrogens by manganese oxides, *Water Res.*, 2008, **42**(20), 5038–5044.

51 C. Gu, Y. Chen, Z. Zhang, S. Xue, S. Sun, K. Zhang, *et al.*, Electrochemical Route to Fabricate Film-Like Conjugated Microporous Polymers and Application for Organic Electronics, *Adv. Mater.*, 2013, **25**(25), 3443–3448.

52 W. Huang, G. Wu, H. Xiao, H. Song, S. Gan, S. Ruan, *et al.*, Transformation of m-aminophenol by birnessite (δ-MnO_2) mediated oxidative processes: Reaction kinetics, pathways and toxicity assessment, *Environ. Pollut.*, 2020, **256**, 113408.

53 J. D. Sivey, M. A. Bickley and D. A. Victor, Contributions of BrCl, Br_2, BrOCl, Br_2O, and HOBr to regiospecific bromination rates of anisole and bromoanisoles in aqueous solution, *Environ. Sci. Technol.*, 2015, **49**(8), 4937–4945.

54 K. Huang, K. P. Reber, M. D. Toomey, J. A. Howarter and A. D. Shah, Reactivity of the polyamide membrane monomer with free chlorine: Role of bromide, *Environ. Sci. Technol.*, 2021, **55**(4), 2575–2584.

55 H. Zhang and C.-H. Huang, Oxidative transformation of triclosan and chlorophene by manganese oxides, *Environ. Sci. Technol.*, 2003, **37**(11), 2421–2430.

56 Z. Hao, F. Shi, D. Cao, J. Liu and G. Jiang, Freezing-induced bromate reduction by dissolved organic matter and the formation of organobromine compounds, *Environ. Sci. Technol.*, 2020, **54**(3), 1668–1676.

57 J. T. Swenson, M. Ginder-Vogel and C. K. Remucal, Influence of divalent cation inhibition and dissolved organic matter enhancement on phenol oxidation kinetics by manganese oxides, *Environ. Sci. Technol.*, 2024, **58**(5), 2479–2489.

58 S. Zhang, J. Lv, R. Han, Z. Wang, P. Christie and S. Zhang, Sustained production of superoxide radicals by manganese oxides under ambient dark conditions, *Water Res.*, 2021, **196**, 117034.

59 M. Altarawneh and B. Z. Dlugogorski, Formation and chlorination of carbazole, phenoxazine, and phenazine, *Environ. Sci. Technol.*, 2015, **49**(4), 2215–2221.

